HHS Public Access

Author manuscript

Results Chem. Author manuscript; available in PMC 2024 November 04.

Published in final edited form as:

Results Chem. 2024 July ; 9: . doi:10.1016/j.rechem.2024.101643.

Azido derivatives of sesquiterpene lactones: Synthesis, anticancer proliferation, and chemistry of nitrogen-centered radicals

Yahaira Reyes[a], **Enoch K. Larrey**[b], **Rupak Pathak**[b], **Maria L. Veisaga**[c], **Manuel A. Barbieri**[c], **Samuel Ward**[d], **Anil Kumar**[d], **Michael D. Sevilla**[d], **Amitava Adhikary**[d], **Stanislaw F. Wnuk**[a]

[a]Department of Chemistry and Biochemistry, Florida International University, Miami, Florida 33199, USA;

[b]Department of Pharmaceutical Sciences, Division of Radiation Health, University of Arkansas for Medical Sciences, Little Rock, Arkansas, 72205, USA;

[c]Department of Biological Sciences, Florida International University, Miami, Florida 33199, USA;

[d]Department of Chemistry, Oakland University, Rochester, Michigan 48309, USA.

Abstract

Sesquiterpene lactones (SLs) such as parthenolide (PTL) and dehydroleucodine (DhL) selectively kill cancer cells without exerting normal tissue toxicity, potentially due to presence of α-methylene-γ-lactone (αMγL) fragment. We hypothesize that the addition of an azido group to the αMγL fragment of PTL or DhL further augments their anticancer properties as well as radiation sensitivity of cancer cells. Azido-SLs containing the azido group at the C14 methyl position of PTL (i.e., azido-melampomagnolide B, AzMMB) while preserving the mechanistically crucial exomethylene unit of αMγL fragment were also prepared. Sham-irradiated (i.e., unirradiated control) or irradiated human breast cancer cells (MCF7) were treated with different concentrations of azido-PTL (AzPTL) or azido-DhL (AzDhL) along with parental SLs. Proliferation rate of MCF7 cells were measured by MTT-assay, and their colony forming ability was determined by colony formation assay. Both AzPTL and AzDhL significantly suppress proliferation rate and colony forming ability of MCF-7 cells. AzPTL suppressed colony forming ability, not cellular proliferation, following irradiation to a greater extent than PTL at lower concentrations (5 and 10 μM). Electron spin resonance (ESR) studies were performed employing gamma-irradiated

Corresponding Author: Stanislaw F. Wnuk - Department of Chemistry and Biochemistry, Florida International University, Miami, Florida 33199, United States; wnuk@fiu.edu.

CRediT authorship contribution statement

Yahaira Reyes: Methodology, Investigation, Writing – Original Draft. **Enoch K. Larrey:** Investigation, **Rupak Pathak:** Methodology, Supervision, Funding acquisition, Writing – Original Draft**. Maria L. Veisaga:** Investigation, **Manuel A. Barbieri.** Methodology, Supervision, Writing – Original Draft. **Samuel Ward:** Investigation. **Anil Kumar:** Formal analysis. **Michael D. Sevilla:** Methodology, Funding acquisition. **Amitava Adhikary:** Methodology, Supervision, Funding acquisition, Writing – Original Draft. **Stanislaw F. Wnuk:** Conceptualization, Methodology, Supervision, Writing – Review & Editing.

Declaration of competing interest

The authors declare that they have no known competing financial interests or personal relationships that could have appeared to influence the work reported in this paper.

Supplementary data

Supplementary data to this article can be found online at https://doi. org/10.1016/j.rechem.2024.101643.

homogeneous supercooled aqueous solutions to investigate radical formation through addition of radiation-mediated prehydrated electrons to the azide group of AzPTL and AzDhL and to follow subsequent reactions of these radicals. In AzPTL, formation of a tertiary carbon-centered radical plausibly via a metastable aminyl radical was observed, whereas AzDhL produced both π-aminyl and α-azidoalkyl radicals. These radicals may contribute to the antitumor activities of AzPTL and AzDhL.

Keywords

Aminyl radicals; azides; cellular proliferation; azido parthenolides; dissociative electron attachment; radiation; radiosensitizers; sesquiterpene lactones

1. Introduction

Breast cancer is the second most common cause of death globally and in 2020, 2.3 million women were diagnosed and 685,000 deaths were recorded worldwide.[1] Natural compounds have gained a significant interest in cancer treatment due to their anti-tumor properties with minimum toxicity to healthy tissues. Parthenolide (**1**, PTL), isolated from *Tanacetum parthenium*, and dehydroleucodine (**2**, DhL), isolated from *Artemisia douglasiana*, are sesquiterpene lactones (SLs; see Scheme 2) which can limit cancer cell growth.[2–9] Importantly, both PTL and DhL were shown to exert no toxicity rather protecting the healthy normal cells from various toxic challenges including radiation.[10–12] Attributed to the presence of a α-methylene-γ-lactone group (αMγL), these SLs possess anti-tumor, anti-migraine, anti-inflammatory, antimicrobial, anti-allergic, and anti-diabetic activities.[2, 8, 13–15] These properties are believed to be driven by the modifications of the exocyclic methylene group through Michael addition reactions with transcription factors, cytokines, and proteins such as the nuclear factor κB (NF-κB) complex.[2–4, 16, 17] For example, PTL and its more-bioavailable derivative dimethylamino parthenolide (DMAPTL) have demonstrated radiosensitization in lung and prostate cancer cells via inhibition of NF-κB, caspase-dependent apoptosis, and alteration of intracellular thiol reduction-oxidation chemistry.[18–21]

The azido modified natural products such as azido nucleosides holds promise to kill cancer cells more effectively with radiotherapy because of their oxidizing radical formation ability under reducing environment, thus making the radiation therapy more effective. For example, 3’-azido-3’-deoxythymidine (AZT) enhances the sensitivity of squamous carcinoma, human colon cancer, and malignant glioma cells to radiation.[22–24] Moreover, addition of 5-azidomethyl-2’-deoxyuridine (5-AmdU) makes the EMT6 breast tumor cells more radiosensitive compared to radiation alone.[25] This radiosensitization enhancement is believed to be attributed to the generation of nitrogen centered radicals (NCRs) such as the oxidizing neutral, π-type aminyl radical (RNH•)[25–28] and their subsequent reactions[29–31] known to play an important role in peptide cellular signaling[32–34] and conjugation.[35] Employing a combination of electron spin resonance (ESR) spectroscopy at low temperature, pulse radiolysis at ambient temperature and theoretical calculations, we previously showed that azido-substituted nucleosides and sugars form NCRs specifically at

the site of the azide group via dissociative electron attachment (DEA).[25–28, 36–38] Thus, addition of an electron to the azido group in 5-AmdU forms the highly unstable azide anion radical ($RN_3•^-$) which following facile N_2 loss forms the highly basic nitrene anion radical ($RN•^-$). Both $RN_3•^-$ and $RN•^-$ were not detected by ESR even at 77 K. Subsequent rapid protonation of $RN•^-$ from the surrounding solvent water produces RNH• (Scheme 1), which was detected by ESR at 77 K and pulse radiolysis at room temperature. Due to its reactivity and oxidizing nature, RNH• undergoes a plethora of reactions including formation of a highly unstable α-azidoalkyl radical which facilely converts to a thermodynamically more stable σ-type iminyl radical.[25, 27]

Based on our above-mentioned work on azido-DNA models, we hypothesize that the azido derivatives of PTL and DhL might exert more potent antitumor effects as they generate the oxidizing neutral π-aminyl radical RNH• via dissociative electron attachment (DEA) pathway.[25–28, 36] To date, the efficacy of RNH• formed from azido sesquiterpene lactones via DEA has not been tested; however, the augmentation of radiation damage to cancerous cells via electron-mediated aminyl/iminyl radicals has already been reported.[25] Herein, we report the synthesis of azido modified sesquiterpene lactones with and without mechanistically crucial exomethylene unit, their anti-tumor efficacy prior to or following exposure to ionizing radiation, and their radical ESR identification in γ-irradiated homogeneous aqueous supercooled (glassy) solutions.

2. Results and Discussion

2.1. Chemical Synthesis

Given that SLs contain the reactive exomethylene group (αMγL), the targeted compounds were synthesized via addition reactions as shown in Scheme 2. Addition of trimethylsilyl azide $TMSN_3$ (in the presence AcOH and Et_3N) to the exomethylene double bond in **1** provided AzPTL **3** in 87% yield. Similarly, treatment of **2** produced AzDhL **4** in 82% yield. Carrying out these reactions in a pressurized vessel under reflux provided better results compared to the reported standard procedures.[6, 39, 40] The improved yields are attributed to the minimal loss of HN_3 with the use of the pressure vessel.

To further study the azido modified SLs, we also prepared a second generation of AzSLs containing the azido group at the C14 methyl position of PTL **1** while preserving the mechanistically crucial exomethylene unit (i.e., azido-melampomagnolide B, AzMMB, **7**; Scheme 3). The conditions for this synthesis must be mild to minimize side reactions including epoxide ring opening and overoxidation of methyl group in **1**. Literature reports difficulty in controlling synthesis of the desired allylic alcohol melampomagnolide B (MMB, **5**) intermediate due to overoxidation of **1** to aldehyde **6**.[41] The overoxidation was observed when employing a Riley-oxidation (1.5 eq SeO_2, dioxane/AcOH, 18 h, 100 °C) which mainly provided aldehyde **6** (56%). However, treatment of PTL **1** via the Sharpless protocol[42] with catalytic SeO_2 in the presence of *tert*-butyl hydroperoxide TBHP (DCM, rt, 24 h) provided MMB **5** (63%) and **6** (10%).[43] Mesylation of **5** followed by displacement with azide provided AzMMB **7** (60%).

2.2. Cellular Proliferation Assays

2.2.1. Azido derivatives of PTL and DhL limit proliferation of MCF-7 cells.—

Treatment with AzPTL and AzDhL in the range of 0 to 20 μM doses for 24 h dependently decreased MCF-7 cells proliferation (Figure 1). Interestingly, the rate of decrease in cellular proliferation were different for AzPTL **3** and AzDhL **4**. For both compounds, the highest anti-proliferative ability was observed at 20 μM, but AzPTL exhibited higher efficacy in limiting the breast cancer cells proliferation than AzDhL and represents a more promising cancer therapeutic candidate. We do not know whether the difference in structural configuration or functional activities are responsible for making AzPTL more effective in controlling breast cancer cells than the AzDhL, which warrant further investigations. However, limiting breast cancer cell proliferation by azido modification to the αMγL of the parent PTL and DhL is a promising step forward in treating breast cancer patients.

2.2.2. Not AzDhL, but AzPTL limits MCF-7 cell proliferation to a greater extent than their respective parent SLs.—

Numerous studies have shown that PTL[44–47] and DhL,[48, 49] have potent anti-breast cancer properties. Similarly, we also found PTL and DhL suppress proliferation rate in MCF-7 cells. However, the efficacy of azido modifications of these parent compounds in limiting breast cancer cell proliferation is not known. Comparison studies revealed that the AzPTL **3** suppresses MCF-7 proliferation to a greater extent than the parent PTL **1** at the concentration of 5 and 10 μM (Figure 2A), while the parent DhL **2** suppresses cell proliferation to a greater extent than the AzDhL **4** (Figure 2B). PTL **1** decreased the proliferation rate of MCF7 cells by approximately 13% and 42% at 5 μM and 10 μM concentrations, respectively, compared to the control group. In contrast, AzPTL **3** displayed a more pronounced inhibitory effect on MCF7 cell proliferation, reducing it by approximately 46% and 60% at the same concentrations (Figure 2A). Similarly, DhL **2** suppressed MCF7 cell proliferation by approximately 22% and 36% at 5 μM and 10 μM concentrations, while AzDhL **4** showed a milder suppression effect, reducing proliferation by approximately 15% and 25%, respectively (Figure 2B). These results of MTT assay after 24 h of incubation showed that AzPTL **3** was more potent than the parent **1** in restricting the breast cancer cells proliferation, while AzDhL **4** exhibited less anti-proliferative ability than the parent **2**. Earlier studies also exhibit a decline in proliferation capacity of MCF-7 cells treated with DhL,[48, 49] which corroborate our current findings.

2.2.3. Azido derivatives of both PTL and DhL do not further enhance sensitivity of MCF-7 cells to radiation.—

Although the radio-sensitizing efficacy of parent DhL is not known, a previous study demonstrated that parent PTL enhances cellular radiosensitivity by inhibiting the NF-κB pathway.[18] Notably, the efficacy of azido PTL and azido DhL in enhancing radiosensitivity is unknown. We also investigated the ability of AzPTL **3** and AzDhL **4** in enhancing radiosensitivity as compared to their respective parent compounds PTL **1** and DhL **2** with an MTT assay. MCF-7 cells were treated with 2.5 μM of either parent SLs or AzPTL **3** and AzDhL **4** for 30 minutes before exposure to 2 Gy irradiation and then the cells were allowed to grow in the drug containing media for 24 h. Compared to the PTL **1** and DhL **2**, both AzPTL **3** and AzDhL **4** did not further enhance sensitivity of MCF-7 cells to a greater extent (Figure 3A and 3B). Earlier studies showed

that PTL-mediated inhibition of the NF-κB pathway enhances radiosensitivity of cancer cells[19,50]. The differences observed for **3** and **4** might be attributed to the different radical species generated (e.g., **9** from **3** and **10** or **11** from **4**).

2.2.4. Co-exposure to AzPTL and radiation limits colony forming ability of MCF-7 cells to a greater extent than the singular treatments.—MCF-7 cells were exposed to 2 Gy radiation and allowed to grow in presence or absence of AzPTL **3** (0.8 μM) at a density of 1,000 cells/well in 6-well plate for 10 days. The colony forming ability in different groups were determined visually following Crystal violet staining. Although the visible colonies of regular size were formed in the sham-irradiated untreated group, 2 Gy irradiation significantly decreased the colony size and number of visible colonies, while microscopic micro colonies were formed in AzPTL and AzPTL plus radiation group, which are invisible to the naked eye. However, the number of microscopic micro colonies were significantly lower in AzPTL plus radiation treated group as compared to AzPTL-treated group without radiation. Because no visible colonies were formed in AzPTL and AZPTL plus radiation treated groups, we presented qualitative data of clonogenic survival assay by capturing images under 4x magnification (Figure 4). Similar colonies formation was observed for treatment with AzDhL.

2.2.5. NAC reverses the inhibitory effect of SLs and azido-SLs in MCF-7 cell.—To correlate the cell proliferative effects and oxidative damage observed for the MCF-7 cell, in the absence of radiation, an *N*-acetylcysteine (NAC) reverse-inhibition study was performed. As demonstrated in Figure 5, MCF-7 cells treated with PTL **1** and AzPTL **3** (Chart A) or DhL **2** and AzDhL **4** (Chart B) without the addition of NAC, had decreased cellular proliferation. However, when MCF-7 cells were subjected to both **1**–**4** and NAC, the cell proliferative effect was blocked (reversed) demonstrating a direct correlation of the SLs oxidative damage.[18, 20]

2.2.6. Azido-SLs limit proliferation of MDA-MB-231 cell.—The AzSLs and parent SLs derivatives were also assayed in MDA-MB-231 cells (Figure 6). As expected, the addition of NAC did not affect the proliferation rate of MDA-MB-231. PTL **1** and AzPTL **3** demonstrated a lower cell proliferative rate (graph A). A similar trend was observed for DhL **2** and AzDhL **4** (graph B). A NAC study of the parental SLs (PTL, DhL) versus their azide derivatives (AzPTL, AzDhL) further supports a direct correlation of MDA-MB-231 cellular proliferation with oxidative damage. The parental SLs and azido SLs demonstrated comparable suppression of MDA-MB-231 cell proliferation rates and reversal upon treatment with NAC.

2.2.7. Cellular proliferation assays with azido-melampomagnolide B

AzMMB limits colony formation ability of MCF-7 cells to a greater extent than PANC-1 and MDA-MB-231 cells.: To evaluate the efficacy of the 2nd generation azido modified sesquiterpene lactone, three cancer cell lines such as MCF-7, MDA-MB-231, and PANC-1 were treated with various doses of AzMMB **7** for three different time intervals. AzMMB treatment suppressed cell proliferation for all three cancer cell lines at 24 h, 48 h (Figure S1), and 72 h (Figure 7). However, the magnitude of decline in cellular proliferation

was greater in MCF-7 cells as compared to MDA-MB-231 and PANC-1 cell lines. Images of cell morphology (Figure S2) confirm these trends.

AzMMB demonstrates anti-clonogenic potential against MCF-7, MDA-MB-231 and PANC-1 cells.: Treatment with 5 μM AzMMB **7** significantly declined the colony forming ability of MCF-7, MDA-MB-231, and PANC-1 cancer cell lines (Figure S3). Like cell proliferation data, the magnitude of the colony forming ability was significantly lower in MCF-7 cells as compared to MDA-MB-231 and PANC-1 cell lines.

The differences in the MCF-7 cell proliferative inhibition of 1st generation versus 2nd generation azido modified SLs is likely attributed to the structural differences of these derivatives compared to PTL. Although the αMγL moiety is intact in AzMMB (2nd generation), the addition of the azide to the C14 carbon decreased the antiproliferative capacity of AzMMB compared to PTL and AzPTL (1st generation; Fig. 1A and 2A versus Fig. 7A and S1).

2.3. ESR Studies and Theoretical Calculations

2.3.1. Studies with AzPTL 3—ESR studies to elucidate the chemical pathways of radiosensitization provided by these SLs were performed in γ-irradiated glassy homogeneous solutions of AzPTL and AzDhL (7.5 M LiCl/D_2O for AzPTL **3**, 7.5 M LiBr/D_2O for AzDhL **4**). Figure 8A shows the ESR spectrum (black) obtained after addition of radiation-mediated prehydrated electrons to AzPTL **3** at 77 K (after subtraction of the line components of $Cl_2^{\bullet-}$). Employing hyperfine coupling constants (HFCC) of three β-protons (see discussion of Figure S4 in SI section) and a *g*-value (2.0032) a simulated spectrum (red) is obtained, which matches the experimental spectrum (black). Moreover the *g*-value of the center of the black spectrum (2.0032) matches with the g-value (2.0032) that we reported for a tertiary C-centered sugar radical, C3′•, obtained via photoexcitation of guanine cation radical ($G^{\bullet+}$) from 2'-deoxyguanosine (see Figure S4)[51] Thus, contrary to our previous detection of RNH• from azidonucleosides and azidosugars (see Scheme 1),[25–28] formation of a neutral tertiary carbon-centered aminomethyl-PTL• radical (AmPTL• **9**) with three β-H HFCC was observed (Scheme 4).

Surprisingly, ESR studies, even at 77 K, could not detect the expected aminyl radical intermediate PTL-NH• **8** from **3** indicating formation of **9** occurs via a facile intramolecular H atom transfer in **8** through a favorable 4-membered ring transitional state (Scheme 4). Annealing of this sample to ca, 145 K and to ca. 155 K in the dark produced the black spectra shown in Figures 8B and 8C which aligns with the red simulated spectrum (Figure 8C). Comparison of the experimentally and theoretically obtained HFCC values employing DFT/B3LYP-PCM/6–31G** method provide additional support to our assignment of the C-centered radical **9** (see SI Section for detailed discussion and Figure S6).

Analyses of the spectra in Figures 8A and 8C shows a temperature-dependent increase of the total hyperfine splitting attributed to the conformational relaxation that leads to change of the HFCC of the β-protons in **9**. We note here that, tertiary C-centered radicals (e.g., C3'•) observed in nucleosides also contributed to different β-proton HFCC values when temperature and base varied,[26, 52–54] thereby, aiding further support to our assignment

of radical **9**. Reducing the concentration of AzPTL by a factor of 2 did not show any observable effect on the ESR spectra shown in Figure 8 confirming that formation of **9** occurred intramolecularly.

2.3.2. Studies with DhL 4—Radiation-produced electron addition to AzDhL **4** allowed us to identify the π-aminyl radical (DhL-NH•) **10** and α-azidoalkyl radical (R-CH(•)-N_3) **11** (Figure 9 and Scheme 5). The red spectrum in Figure 9A shows three important characteristics: (i) the outermost hyperfine structures due to a single axially symmetric anisotropic nitrogen with HFCC and *g*-values that are typical to a neutral aminyl radical nitrogen in **10**[25–28]; (ii) a broad central doublet of ca. 84 G similar to the reported for the aminyl radical generated in our azido nucleosides[25–27]; and (iii) the match between the experimentally recorded spectrum (red) and the simulated spectrum (violet) establishes that the central multiplet arises from aminyl radical **10** and carbon-centered radical **11**. Subsequent warming of this sample for 15 min in the dark to ca. 145 K and 150 K led to the red spectra shown in Figures 9B and 9C (See SI Section for detailed discussion and simulation parameters of the radicals; Figures S5 and S7–S9). Comparison of the spectra in Figure 9 shows that contrary to our previous observations of σ-iminyl radical formation,[25, 27] we only detect the π-aminyl radical **10** and α-azidoalkyl radical **11** species with AzDhL **4**. This is because the expected doublet due to the isotropic β-H HFCC ca. 80 G of the σ-iminyl radical (R-CH=N•; e.g., **12**), observed in our previous work,[25, 27, 55] was not observed in spectrum C in the glassy system.

AzPTL **3** and AzDhL **4** have the common structure R-CH_2-N_3; therefore, based on our previous studies,[25, 27] the formation σ-type iminyl radicals such as **12** is expected in both **3** and **4**. However, comparison of the ESR spectral results in Figures 8 and 9 show that the conformation of aminyl radicals dictate the subsequent radical formation – i.e., formation of a tertiary C-centered radical **9** in AzPTL **3** and the aminyl radical **10** and α-azidoalkyl radical **11** in AzDhL **4**. The role of C-centered radicals in causing radiosensitization is well-established in the literature through H-atom abstraction leading to sugar radical formation that are precursors of strand break and unaltered nucleobase release[28, 29, 51–54] Since our previous works and the literature established that aminyl radicals are well-known oxidizers[25–29, 31] we predict that both AzPTL **3** and AzDhL **4** could be better radiosensitizers than their parent compounds as they generate NCRs. Radical species from **3** and **4** are also expected to have a better solubility in water than their azido precursors.

2. Conclusions

Addition of trimethylsilyl azide to the exomethylene double bond in SLs **1** and **2** in the presence AcOH and Et_3N provided AzPTL **3** and AzDhL **4**derivatives with a modified αMγL group. Oxidation of C14 methyl group in PTL **1** to hydroxymethyl and conversion to azidomethyl unit provided azido-melampomagnolide B, (AzMMB, **7**) while preserving the mechanistically crucial exomethylene unit. Addition of radiation-produced electrons to AzPTL **3** leads to formation of an aminyl radical which transforms into a tertiary C-centered radical AmPTL• **9**; whereas radiation-mediated electron addition to AzDhL **4** produced the highly reactive oxidizing aminyl radical **10** and α-azidoalkyl radical **11**.

AzPTL and AzDhL significantly suppressed proliferation rate and colony forming ability in MCF-7 cells. Notably, AzPTL in combination with radiation restricted colony forming ability to a greater extent than the singular treatments. The radiosensitization observed for these azido-SLs might be attributed to the increased reactive oxygen species (ROS) generated via radicals **9**, **10** or **11** and is also supported by NAC reversal effect on the activity of these compounds as C- and N-centered radicals can be effective in augmenting radiation damage.[25–29, 51–55] These results could provide additional support to finding that DMAPTL-induced radiosensitization might occur via two possible pathways (a) inhibition of intracellular thiol redox chemistry, and (b) inhibition of the NF-κB pathway.[21] Our findings involve the combination of synthesis, ESR, theoretical calculations as well as biochemical and cellular studies and provide insight to the higher radiosensitization shown by azido-SLs than the parent SLs.

4. Experimental Part

4.1. Synthetic and spectroscopic data

Parthenolide PTL **1** and dehydroleucodine DhL **2** were purchased from Ambeed. DhL was also isolated from and purified as described in the literature.[9] All reactions were carried out under argon atmosphere using dry, freshly distilled solvents under anhydrous conditions. Solvents were purified and dried utilizing standard procedures. Reactions were monitored via thin-layer chromatography detected with a 254 nm lamp and stained using $Ce(SO_4)_2$/$(NH_4)_6Mo_7O_{24}{\cdot}4H_2O$/$H_2SO_4$/$H_2O$ reagent or I_2 chamber. Reported are isolated yields after purification via column chromatography using Merck silica gel 60 (230 – 400 mesh). ^1H and ^{13}C NMR were obtained using a Bruker 400 MHz instrument with solutions of $CDCl_3$.

Azidoparthenolide (AzPTL) **3**. To a pressure vessel equipped with a stir bar, at rt, under N_2, DCM (5 mL) was added followed by AcOH (0.23 mL, 4.03 mmol, 9.9 eq), and TMS-N_3 (0.5 mL, 4.03 mmol, 9.9 eq). After 30 minutes, PTL **1** (101.0 mg, 0.41 mmol, 1 eq) and Et_3N (0.01 mL, 0.08 mmol, 0.2 eq) were sequentially added and reaction was placed in a 40 °C oil bath and stirred overnight. Reaction was cooled to rt and evaporated under reduced pressure. The residue was purified using (EtOAc/hexane; 20:80 → 40:60) to give **3**[6] (103 mg, 87%) as a white solid: ^1H NMR δ 1.19–1.27 (m, 1H), 1.30 (s, 3H), 1.70 (m, 4H) 1.88–1.93 (m, 1H), 2.06 – 2.51 (m, 7H), 2.75 (d, *J* = 9.0 Hz, 1H), 3.62–3.66 (dd, *J* = 3.6 Hz, *J* = 12.8 Hz, 1H), 3.83 – 3.89 (m, 2H), 5.21 (d, *J* =10.6 Hz, 1H); ^{13}C NMR δ 16.9, 17.2, 24.0, 29.7, 36.5, 40.9, 45.9, 47.7, 48.2, 61.5, 66.2, 82.4, 125.3, 134.2, 174.2.

Azidodehydroleucodine (AzDhL) **4**. To a pressure vessel equipped with a stir bar, at rt, under N_2, DCM (5 mL) was added followed by AcOH (14.0 μL, 0.245 mmol, 4.8 eq) and TMS-N_3 (38.0 μL, 0.29 mmol, 5.6 eq). After30 minutes, DhL **2** (12.4 mg, 0.05 mmol, 1 eq) and Et_3N (1.4 μL, 0.01 mmol, 0.2 eq) were sequentially added and reaction was placed in a 40 °C oil bath and stirred overnight. Reaction was cooled to rt and evaporated under reduced pressure. The residue was purified using (EtOAc/hexane; 20:80 → 40:60) to give **4** (11.9 mg, 82%) as a white solid: ^1H NMR δ 1.32 – 1.42 (m, 1H), 2.02 – 2.07 (m, 1H) 2.28 (s, 3H), 2.30 – 2.37 (m, 2H), 2.39 – 2.45 (m, 5H), 3.45 (d, *J* = 10.0 Hz, 1H), 3.62 – 3.69 (m, 2H), 3.78 – 3.83 (dd, *J* = 4.0 Hz, *J* = 12.8 Hz, 1H), 6.16 (m, 1H); ^{13}C NMR δ 19.9, 21.7, 25.9, 37.4, 46.3, 47.9, 51.1, 52.5, 84.3, 131.8, 135.8, 152.2, 169.7, 174.2, 195.8; HRMS:

m/z calcd. $C_{15}H_{17}N_3O_3$ $[M]^+$ 287.1270 found $[M+H]^+$ 288.13482, $[M+Na]^+$ 310.11656, and $[M+K]^+$ 326.09079.

Melampomagnolide B (MMB) **5**. To a pressure vessel equipped with a stir bar, at rt, under Ar, SeO_2 (6.3 mg, 0.057 mmol) was added and purged for 2 min. DCM (4 mL) followed by TBHP (0.02 mL, 0.12 mmol) were sequentially added and stirred for 30 min. A solution of PTL **1** (30.1 mg, 0.12 mmol) in DCM (3 mL) was then added, and reaction was stirred for 24 h. Volatiles were evaporated and residue was purified using (EtOAc/hexane; 0:100 → 70:30) to give **5**[41] (20.1 mg, 63%) as a white solid along with aldehyde **6** (2.6 mg, 10%). Compound **5** had: ^{1}H NMR 1.09 (t, *J* = 12.2 Hz, 1H), 1.60–1.72 (m, 4H), 2.12–2.34 (m, 3H), 2.41 (m, 3H), 2.85 (d, *J* = 9.4 Hz, 2H), 3.85 (t, *J* = 9.3 Hz, 1H), 4.12 (dd, *J* = 12.6, 34.5 Hz, 2H), 5.54 (d, *J* = 3.20 Hz, 1H), 5.65 (t, *J* = 8.24, 1H), 6.23 (d, *J* = 3.5 Hz, 1H). Aldehyde **6** had: ^{1}H NMR δ 1.22–1.26 (m, 1H), 1.58–1.66 (m, 4H), 2.30–2.43 (m, 2H), 2.46–2.64 (m, 4H), 2.72 (d, *J* = 9.5 Hz, 1H), 2.92–3.01 (m, 1H), 3.79 (t, *J* = 9.4 Hz, 1H), 5.57 (d, *J* = 3.2 Hz, 1H), 6.22 (d, *J* = 3.5 Hz, 1H), 6.68 (dt, J = 1.6, 9.4 Hz, 1H), 9.49 (d, *J* = 1.8 Hz, 1H).

AzidoMelampomagnolide B (AzMMB) **7**. *Step a*. Mesylation. Et_3N (0.02 mL, 0.16 mmol) was added to a solution of **5** (16.9 mg, 0.064 mmol) in DCM (5 mL) at rt under Ar. To this solution, MsCl (0.01 mL, 0.13 mmol) was added dropwise and stirred for 1 h. Mixture was then partitioned between ice water and DCM. The organic layer was dried with Na_2SO_4 and volatiles were evaporated. The residue was dried further under reduced pressure and provided the mesylate which was of sufficient purity (TLC) to be directly used in the next step.

Step b. Azidation. NaN_3 (6.24 mg, 0.096 mmol) was added to a solution of crude mesylate from *step a* in DMF (4 mL) at rt under Ar. After 2 h, volatiles were evaporated and residue was column chromatographed (hexane/EtOAc; 100:0→60:40) to give **7**[56] (11.1 mg, 60%) as a white solid. ^{1}H NMR δ 1.12 (t, *J* = 13.0 Hz, 1H), 1.55 (s, 3H), 1.71 (m, 1H), 2.15–2.49 (m, 6H), 2.71–2.75 (m, 1H), 2.84 (d, *J* = 9.3 Hz, 1H), 3.68 (d, *J* = 13.3 Hz, 1H), 3.81–3.87 (m, 2H), 5.55–5.56 (m, 1H), 5.67 (t, *J* = 8.3 Hz, 1H), 6.25–6.27 (m, 1H); ^{13}C NMR ($CDCl_3$, 400 MHz) δ 17.9,23.7, 24.1, 25.3, 36.6, 42.7, 55.6, 59.9, 63.3, 80.9, 120.3, 131.2, 138.6, 169.2.

4.2. Cellular proliferation assays

4.2.1. Without ionizing radiation—The rate of cellular proliferation was determined by MTT assay using a kit from Sigma-Aldrich, Inc. (St. Louis, Missouri). A total of 5 × 10^3 MCF-7, PANC-1, or MDA-MB231 cells were seeded in each well of a 96-well plate with 100 μL of Dulbecco's Modified Eagle Medium (Thermo Fisher Scientific, Waltham, Massachusetts). After 24 hours incubation, 50 μl of fresh media with different concentrations of drug or DMSO was added to each well and further incubated. After 24, 48, or 72 h of drug treatment 10 μL of the labelling agent was added to the wells and incubated for 4 hrs. Then 100 μL of solubilization agent was added and incubated at 37 °C in a humidified CO_2 incubator for overnight. Absorbance was subsequently read at 570 nm with a microplate reader.

3.2.2. With ionizing radiation—The rate of cellular proliferation was determined by MTT assay using a kit from Sigma-Aldrich, Inc. (St. Louis, Missouri). A total of 5 ×

10^3 MCF-7 cells were seeded in each well of a 96-well plate with 100 μL of Dulbecco's Modified Eagle Medium (Thermo Fisher Scientific, Waltham, Massachusetts). After 24 hours incubation, 50 μL of fresh media with different concentrations of drug or DMSO was added to each well and further incubated for 30 minutes before exposure to 2 Gy γ-rays at a dose rate of 0.98 Gy/minute. After 24 h of irradiation 10 μL of the labelling agent was added to the wells and incubated for 4 hrs. Then 100 μL of solubilization agent was added and incubated at 37 °C in a humidified CO_2 incubator overnight. Absorbance was subsequently read at 570 nm with a microplate reader.

3.2.3. Colony formation assay—A total of 1×10^3 cells were seeded with 3 mL of Dulbecco's Modified Eagle Medium in each well of a 6-well plate. After 6 hours of incubation, the seeding medium was replaced with fresh medium containing either 0.8 μM drug or DMSO. After 30 minutes of drug treatment the 6-well plates were exposed to 2 Gy γ-rays at a dose rate of 0.98 Gy/minute. Cells were then incubated for 10 days in a humidified CO_2 incubator. After 10 days the medium was discarded, and all the wells were washed with 1× PBS. Colonies were fixed with 70% alcohol for 15 minutes, and then stained with 0.1 % crystal violet solution. Excess crystal violet solution was washed with distilled water and the wells were left to dry. Colonies with more than 50 cells were considered as regular colonies, while colonies with less than 50 cells were considered as micro-colonies. Most of the micro-colonies were invisible to the naked eye and were visualized under 4× magnification.

3.2.4. NAC Study Description—Cells (MCF-7 or MBA-MD-231, 2×10^5) were seeded and incubated for 24 h. After incubation, cells were treated with (10 μM) of selected SLs or AzSLs (**1–4**) as shown in the Figures 5 and 6 in the absence or presence of 2 mM NAC for an additional 24 h. At the end of the second incubation, cells were washed with PBS and 2 mL serum-free culture medium containing 1 mg/mL MTT [3-(4,5-dimethylthiazol-2-yl)-2,5-diphenyltetrazolium bromide; Sigma-Aldrich] was added to each well. The medium was discarded after 6 h, DMSO was added to dissolve MTT-derived formazan, and formazan was quantified by the measurement of absorbance at wavelength 570 nm as previously described.[9]

4.3. ESR Studies and Theoretical Calculations

Calculations employing DFT/B3LYP-PCM/6–31G** method as well as preparation of transparent homogeneous glassy samples, their irradiation and ESR studies as well as analyses of the ESR spectra[28, 51] are detailed in the Supplementary Materials.

Supplementary Material

Refer to Web version on PubMed Central for supplementary material.

Acknowledgements

We thank you Dr. L. A. Lopez from Universidad Nacional de Cuyo, Argentina for providing us a sample of DhL for our initial experiments. SW, AK, MDS, and AA thank the National Cancer Institute of the National Institutes of Health (Grant RO1CA045424) for support. AA thanks the National Science Foundation under Grant No. CHE-1920110. This study was also partly supported by the National Institute of General Medical Sciences

(NIGMS) under Grant No. P20GM109005 (R.P) and NASA Established Program to Stimulate Competitive Research (NASA EPSCoR), under Grant No. 80NSSC21M0323 (R.P).

Data availability

Data will be made available on request

Abbreviations

SLs	Sesquiterpene lactones
PTL	parthenolide
AzPTL	azido-parthenolide
DhL	dehydroleucodine
AzDhL	azido-dehydroleucodine
NF-κB	nuclear factor κB
AZT	3’-azido-3’-deoxythymidine
5-AmdU	5-azidomethyl-2’-deoxyuridine
DMAPTL	dimethylamino parthenolide
AmPTL	aminomethyl parthenolide
αMγL	α-methylene-γ-lactone
ROS	reactive oxygen species
DEA	dissociative electron attachment
ESR	electron spin resonance
HFCC	hyperfine coupling constants
MMB	Melampomagnolide B
AzMMB	AzidoMelampomagnolide

REFERENCES

1. WILD CP; WEIDERPASS E; STEWART BW World Cancer Report; 978-92-832-0448-02020. https://shop.iarc.fr/products/world-cancer-report-cancer-research-for-cancer-prevention-pdf
2. Ordóñez PE; Mery DE; Sharma KK, et al. , Synthesis, Crystallography, and Anti-Leukemic Activity of the Amino Adducts of Dehydroleucodine. Molecules 2020; 25: 4825–4840. 10.3390/molecules25204825 [PubMed: 33092263]
3. Freund RRA; Gobrecht P; Fischer D, et al. , Advances in chemistry and bioactivity of parthenolide. Nat. Prod. Rep 2020; 37: 541–565. 10.1039/C9NP00049F [PubMed: 31763637]
4. Coricello A; Adams DJ; Lien JE, et al. , A Walk in Nature: Sesquiterpene Lactones as Multi-Target Agents Involved in Inflammatory Pathways. Curr. Med. Chem 2020; 27: 1501–1514. 10.2174/0929867325666180719111123 [PubMed: 30027844]

5. Taleghani A; Nasseri MA; Iranshahi M, Synthesis of dual-action parthenolide prodrugs as potent anticancer agents. Bioorg. Chem 2017; 71: 128–134. 10.1016/j.bioorg.2017.01.020 [PubMed: 28215600]
6. Zhang Q; Lu Y; Ding Y, et al. , Guaianolide sesquiterpene lactones, a source to discover agents that selectively inhibit acute myelogenous leukemia stem and progenitor cells. J. Med. Chem 2012; 55: 8757–8769. 10.1021/jm301064b [PubMed: 22985027]
7. Polo LM; Castro CM; Cruzado MC, et al. , 11,13-dihydro-dehydroleucodine, a derivative of dehydroleucodine with an inactivated alkylating function conserves the anti-proliferative activity in G2 but does not cause cytotoxicity. Eur. J. Pharmacol 2007; 556: 19–26. 10.1016/j.ejphar.2006.10.049 [PubMed: 17134695]
8. Kim DY; Choi BY, Costunolide—A bioactive sesquiterpene lactone with diverse therapeutic potential. Int. J. Mol. Sci 2019; 20: 2926–2947. 10.3390/ijms20122926 [PubMed: 31208018]
9. Priestap HA; Galvis A; Rivero N, et al. , Dehydroleucodine and dehydroparishin-B inhibit proliferation and motility of B16 melanoma cells. Phytochem. Lett 2012; 5: 581–585. 10.1016/j.phytol.2012.05.018
10. Morel KL; Ormsby RJ; Bezak E, et al. , Parthenolide Selectively Sensitizes Prostate Tumor Tissue to Radiotherapy while Protecting Healthy Tissues In Vivo. Radiat. Res 2017; 187: 501–512. 10.1667/rr14710.1 [PubMed: 28398879]
11. Morel KL; Ormsby RJ; Klebe S, et al. , DMAPT is an Effective Radioprotector from Long-Term Radiation-Induced Damage to Normal Mouse Tissues In Vivo. Radiat. Res 2019; 192: 231–239. 10.1667/rr15404.1 [PubMed: 31095445]
12. Vera ME; Mariani ML; Aguilera C, et al. , Effect of a Cytoprotective Dose of Dehydroleucodine, Xanthatin, and 3-Benzyloxymethyl-5H-furan-2-one on Gastric Mucosal Lesions Induced by Mast Cell Activation. Int J Mol Sci 2021; 22: 5982–5994. 10.3390/ijms22115983 [PubMed: 34205983]
13. Abood S; Eichelbaum S; Mustafi S, et al. , Biomedical Properties and Origins of Sesquiterpene Lactones, with a Focus on Dehydroleucodine. Nat. Prod. Commun 2017; 12: 995–1005. 10.1177/1934578×1701200638
14. Li Q; Wang Z; Xie Y, et al. , Antitumor activity and mechanism of costunolide and dehydrocostus lactone: Two natural sesquiterpene lactones from the Asteraceae family. Biomed. Pharmacother 2020; 125: 109955–109967. 10.1016/j.biopha.2020.109955 [PubMed: 32014691]
15. Moujir L; Callies O; Sousa PMC, et al. , Applications of Sesquiterpene Lactones: A Review of Some Potential Success Cases. Applied Sciences 2020; 10: 3001–3033. 10.3390/app10093001
16. Chadwick M; Trewin H; Gawthrop F, et al. , Sesquiterpenoids Lactones: Benefits to Plants and People. Int. J. Mol. Sci 2013; 14: 12780–12805. 10.3390/ijms140612780 [PubMed: 23783276]
17. Sztiller-Sikorska M; Czyz M, Parthenolide as Cooperating Agent for Anti-Cancer Treatment of Various Malignancies. J. Pharm 2020; 13: 194–224. 10.3390/ph13080194
18. Mendonca MS; Chin-Sinex H; Jaime G-M, et al. , Parthenolide Sensitizes Cells to X-ray-Induced Cell Killing through Inhibition of NF-κB and Split-Dose Repair. Radiat. Res 2007; 168: 689–697. http://www.jstor.org/stable/4540785 [PubMed: 18088190]
19. Watson C; Miller DA; Chin-Sinex H, et al. , Suppression of NF-κB Activity by Parthenolide Induces X-Ray Sensitivity through Inhibition of Split-Dose Repair in TP53 Null Prostate Cancer Cells. Radiat. Res 2009; 171: 389–396. 10.1667/rr1394.1 [PubMed: 19397439]
20. Siriwan D; Naruse T; Tamura H, Effect of epoxides and α-methylene-γ-lactone skeleton of sesquiterpenes from yacon (Smallanthus sonchifolius) leaves on caspase-dependent apoptosis and NF-κB inhibition in human cercival cancer cells. Fitoterapia 2011; 82: 1093–1101. 10.1016/j.fitote.2011.07.007 [PubMed: 21787849]
21. Mendonca MS; Turchan WT; Alpuche ME, et al. , DMAPT inhibits NF-κB activity and increases sensitivity of prostate cancer cells to X-rays in vitro and in tumor xenografts in vivo. Free Radic. Biol. Med 2017; 112: 318–326. 10.1016/j.freeradbiomed.2017.08.001 [PubMed: 28782644]
22. Coucke PA; Cottin E; Decosterd LA, Simultaneous alteration of de novo and salvage pathway to the deoxynucleoside triphosphate pool by (E)-2'-Deoxy-(fluoromethylene)cytidine (FMdC) and zidovudine (AZT) results in increased radiosensitivity in vitro. Acta Oncol. 2007; 46: 612–620. 10.1080/02841860601137389 [PubMed: 17562437]

23. Zhou FX; Liao ZK; Dai J, et al. , Radiosensitization effect of zidovudine on human malignant glioma cells. Biochem. Biophys. Res. Commun 2007; 354: 351–356. 10.1016/j.bbrc.2006.12.180 [PubMed: 17223082]
24. Liao ZKZ; F X; Luo ZG, et al. , Radio-activation of hTERT promoter in larynx squamous carcinoma cells: An 'indirected-activator' strategy in radio-gene-therapy. Oncol. Rep 2008; 19: 281–286. 10.3892/or.19.1.281 [PubMed: 18097608]
25. Wen Z; Peng J; Tuttle PR, et al. , Electron-Mediated Aminyl and Iminyl Radicals from C5 Azido-Modified Pyrimidine Nucleosides Augment Radiation Damage to Cancer Cells. Org. Lett 2018; 20: 7400–7404. 10.1021/acs.orglett.8b03035 [PubMed: 30457873]
26. Adhikary A; Khanduri D; Pottiboyina V, et al. , Formation of Aminyl Radicals on Electron Attachment to AZT: Abstraction from the Sugar Phosphate Backbone versus One-Electron Oxidation of Guanine. J. Phys. Chem. B 2010; 114: 9289–9299. 10.1021/jp103403p [PubMed: 20575557]
27. Mudgal M; Dang T; Sobczak A, et al. , Site of Azido Substitution in the Sugar Moiety of Azidopyrimidine Nucleosides Influences the Reactivity of Aminyl Radicals Formed by Dissociative Electron Attachment. J. Phys. Chem. B 2020; 124: 11357–11370. 10.1021/acs.jpcb.0c08201 [PubMed: 33270461]
28. Mudgal M; Rishi S; Lumpuy DA, et al. , Prehydrated One-Electron Attachment to Azido-Modified Pentofuranoses: Aminyl Radical Formation, Rapid H-Atom Transfer, and Subsequent Ring Opening. J. Phys. Chem. B 2017; 121: 4968–4980. 10.1021/acs.jpcb.7b01838 [PubMed: 28425714]
29. von Sonntag C, Free-radical-induced DNA Damage and Its Repair. Springer-Verlag: Berlin, Heidelberg, 2006. 10.1007/3-540-30592-0
30. Minozzi M; Nanni D; Spagnolo P, From azides to nitrogen-centered radicals: applications of azide radical chemistry to organic synthesis. Eur. J Chem 2009; 15: 7830–7840. 10.1002/chem.200802710
31. Kumar A; Becker D; Adhikary A; Sevilla MD, Reaction of Electrons with DNA: Radiation Damage to Radiosensitization. Int. J. Mol. Sci 2019; 20: 3998–4024. 10.3390/ijms20163998 [PubMed: 31426385]
32. Kerru N; Gummidi L; Maddila S, et al. , A Review on Recent Advances in Nitrogen-Containing Molecules and Their Biological Applications. Molecules 2020; 25: 1909. 10.3390/molecules25081909 [PubMed: 32326131]
33. Dedon PC; Tannenbaum SR, Reactive nitrogen species in the chemical biology of inflammation. Arch. Biochem. Biophys 2004; 423: 12–22. 10.1016/j.abb.2003.12.017 [PubMed: 14989259]
34. Adams L; Franco MC; Estevez AG, Reactive nitrogen species in cellular signaling. Exp. Biol. Med 2015; 240: 711–717. 10.1177/1535370215581314
35. Ahmad Fuaad A; Azmi F; Skwarczynski M, et al. , Peptide Conjugation via CuAAC 'Click' Chemistry. Molecules 2013; 18: 13148–13174. 10.3390/molecules181113148 [PubMed: 24284482]
36. Adjei D; Reyes Y; Kumar A, et al. , Pathways of the Dissociative Electron Attachment Observed in 5- and 6-Azidomethyluracil Nucleosides: Nitrogen (N2) Elimination vs Azide Anion (N3–) Elimination. J. Phys. Chem. B 2023; 127: 1563–1571. 10.1021/acs.jpcb.2c08257 [PubMed: 36780335]
37. Reyes Y; Mebel A; Wnuk SF, 6-azido and 6-azidomethyl uracil nucleosides. Nucleosides Nucleotides Nucl. Acids 2024, 43: 453–471. 10.1080/15257770.2023.2271023
38. Reyes Y; Adhikary A; Wnuk SF, Nitrogen-Centered Radicals Derived from Azidonucleosides. Molecules 2024; 29: 2310. 10.3390/molecules29102310 [PubMed: 38792171]
39. Horstmann TE; Guerin DJ; Miller SJ, Asymmetric Conjugate Addition of Azide to α,β-Unsaturated Carbonyl Compounds Catalyzed by Simple Peptides. Angew. Chem., Int. Ed 2000; 39: 3635–3638. 10.1002/1521-3773(20001016)39:20
40. Guerin DJ; Horstmann TE; Miller SJ, Amine-Catalyzed Addition of Azide Ion to α,β-Unsaturated Carbonyl Compounds. Org. Lett 1999; 1: 1107–1109. 10.1021/ol9909076 [PubMed: 10825962]

41. Neelakantan S; Nasim S; Guzman ML, et al. , Aminoparthenolides as novel anti-leukemic agents: Discovery of the NF-κB inhibitor, DMAPT (LC-1). Bioorg. Med. Chem. Lett 2009; 19: 4346–4349. 10.1016/j.bmcl.2009.05.092 [PubMed: 19505822]

42. Umbreit MA; Sharpless KB, Allylic oxidation of olefins by catalytic and stoichiometric selenium dioxide with tert-butyl hydroperoxide. J. Am. Chem. Soc 1977; 99: 5526–5528. 10.1021/ja00458a072

43. Bommagani S; Ponder J; Penthala NR, et al. , Indole carboxylic acid esters of melampomagnolide B are potent anticancer agents against both hematological and solid tumor cells. Eur. J. Med. Chem 2017; 136: 393–405. 10.1016/j.ejmech.2017.05.031 [PubMed: 28525840]

44. Ge W; Hao X; Han F, et al. , Synthesis and structure-activity relationship studies of parthenolide derivatives as potential anti-triple negative breast cancer agents. Eur. J. Med. Chem 2019; 166: 445–469. 10.1016/j.ejmech.2019.01.058 [PubMed: 30739826]

45. Ghorbani-Abdi-Saedabad A; Hanafi-Bojd MY; Parsamanesh N, et al. , Anticancer and apoptotic activities of parthenolide in combination with epirubicin in mda-mb-468 breast cancer cells. Mol Bio Rep 2020; 47: 5807–5815. 10.1007/s11033-020-05649-3 [PubMed: 32686017]

46. Carlisi D; Lauricella M; D'Anneo A, et al. , The Synergistic Effect of SAHA and Parthenolide in MDA-MB231 Breast Cancer Cells. J. Cell. Physiol 2015; 230: 1276–1289. 10.1002/jcp.24863 [PubMed: 25370819]

47. Carlisi D; Buttitta G; Di Fiore R, et al. , Parthenolide and DMAPT exert cytotoxic effects on breast cancer stem-like cells by inducing oxidative stress, mitochondrial dysfunction and necrosis. Cell Death Dis. 2016; 7: e2194. 10.1038/cddis.2016.94 [PubMed: 27077810]

48. Bailon-Moscoso N; González-Arévalo G; Velásquez-Rojas G, et al. , Phytometabolite Dehydroleucodine Induces Cell Cycle Arrest, Apoptosis, and DNA Damage in Human Astrocytoma Cells through p73/p53 Regulation. PLoS One 2015; 10: e0136527. 10.1371/journal.pone.0136527 [PubMed: 26309132]

49. Costantino VV; Mansilla SF; Speroni J, et al. , The Sesquiterpene Lactone Dehydroleucodine Triggers Senescence and Apoptosis in Association with Accumulation of DNA Damage Markers. PLoS One 2013; 8: e53168. 10.1371/journal.pone.0053168 [PubMed: 23341930]

50. Sun Y; St. Clair DK; Fang F, et al. , The radiosensitization effect of parthenolide in prostate cancer cells is mediated by nuclear factor-κB inhibition and enhanced by the presence of PTEN. Mol. Cancer Ther 2007; 6: 2477–2486. 10.1158/1535-7163.Mct-07-0186 [PubMed: 17876045]

51. Adhikary A; Malkhasian AYS; Collins S, et al. , UVA-visible photo-excitation of guanine radical cations produces sugar radicals in DNA and model structures. Nucleic Acids Res. 2005; 33: 5553–5564. 10.1093/nar/gki857 [PubMed: 16204456]

52. Adhikary A; Becker D; Collins S, et al. , C5′- and C3′-sugar radicals produced via photo-excitation of one-electron oxidized adenine in 2′-deoxyadenosine and its derivatives. Nucleic Acids Res. 2006; 34: 1501–1511. 10.1093/nar/gkl026 [PubMed: 16537838]

53. Adhikary A; Collins S; Khanduri D, et al. , Sugar Radicals Formed by Photoexcitation of Guanine Cation Radical in Oligonucleotides. J. Phys. Chem. B 2007; 111: 7415–7421. 10.1021/jp071107c [PubMed: 17547448]

54. Khanduri D; Collins S; Kumar A, et al. , Formation of Sugar Radicals in RNA Model Systems and Oligomers via Excitation of Guanine Cation Radical. J. Phys. Chem. B 2008; 112: 2168–2178. 10.1021/jp077429y [PubMed: 18225886]

55. Adhikary A; Kumar A; Bishop CT, et al. , π-Radical to σ-Radical Tautomerization in One-Electron-Oxidized 1-Methylcytosine and Its Analogs. J. Phys. Chem. B 2015; 119: 11496–11505. 10.1021/acs.jpcb.5b05162 [PubMed: 26237072]

56. Janganati V; Ponder J; Balasubramaniam M, et al. , MMB triazole analogs are potent NF-κB inhibitors and anti-cancer agents against both hematological and solid tumor cells. Eur. J. Med. Chem 2018; 157: 562–581. 10.1016/j.ejmech.2018.08.010 [PubMed: 30121494]

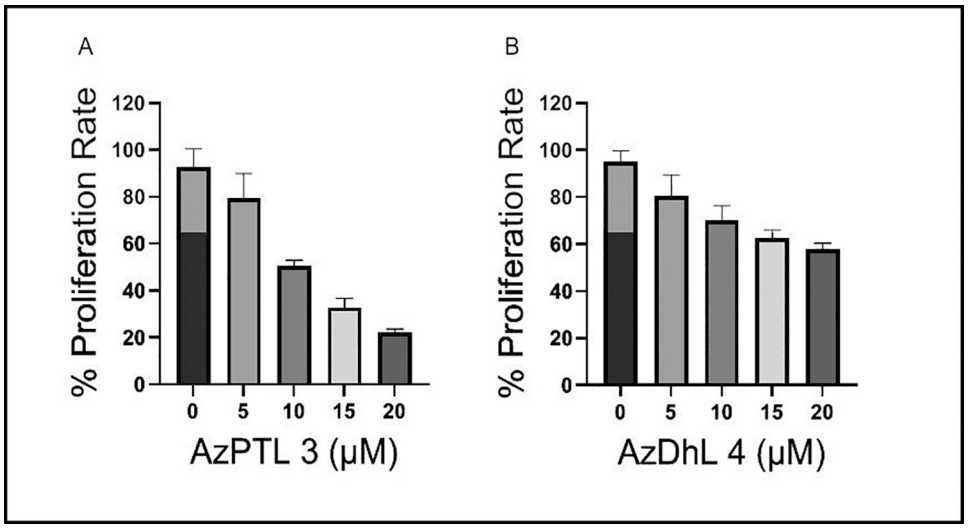

Figure 1.
Dose-dependent decrease in proliferation rate in MCF-7 cells following treatment with (A) AzPTL and (B) AzDhL.

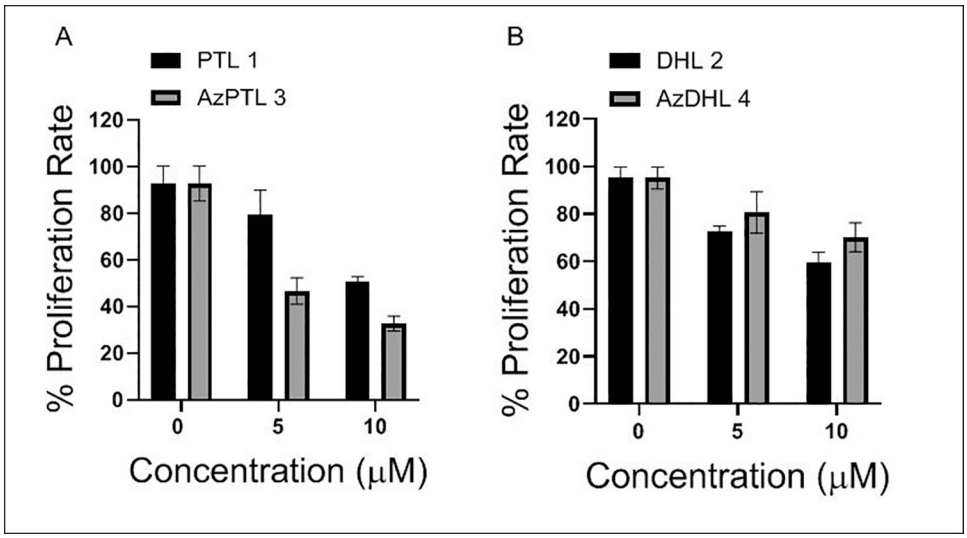

Figure 2.

MTT assay revealed (A) AzPTL **3** suppresses MCF-7 cell proliferation to a greater extent than the PTL **1**, (B) the parent DhL **2** is more effective in checking MCF-7 cell proliferation than the AzDhL **4**.

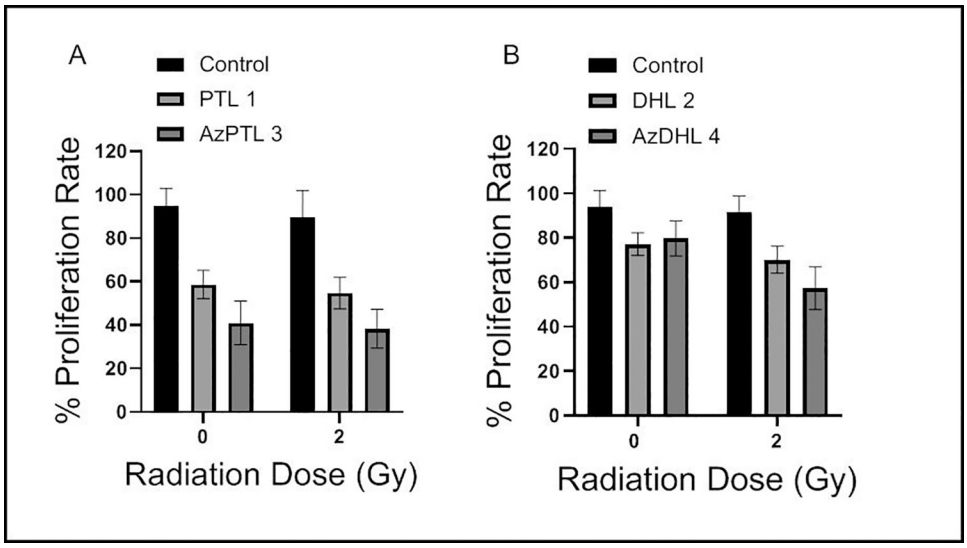

Figure 3.

Treatments with 2.5 μM of (A) PTL **1** or AzPTL **3** and (B) DhL **2** or AzDhL **4** exhibit no further enhancement of anti-proliferative ability following radiation in MCF-7 cells.

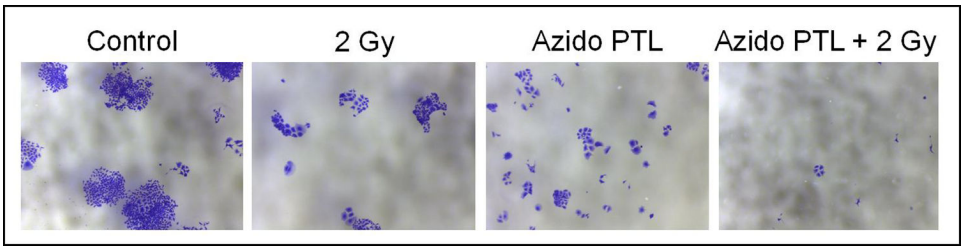

Figure 4.
Representative photomicrographs of MCF-7 colonies in different treatment groups.

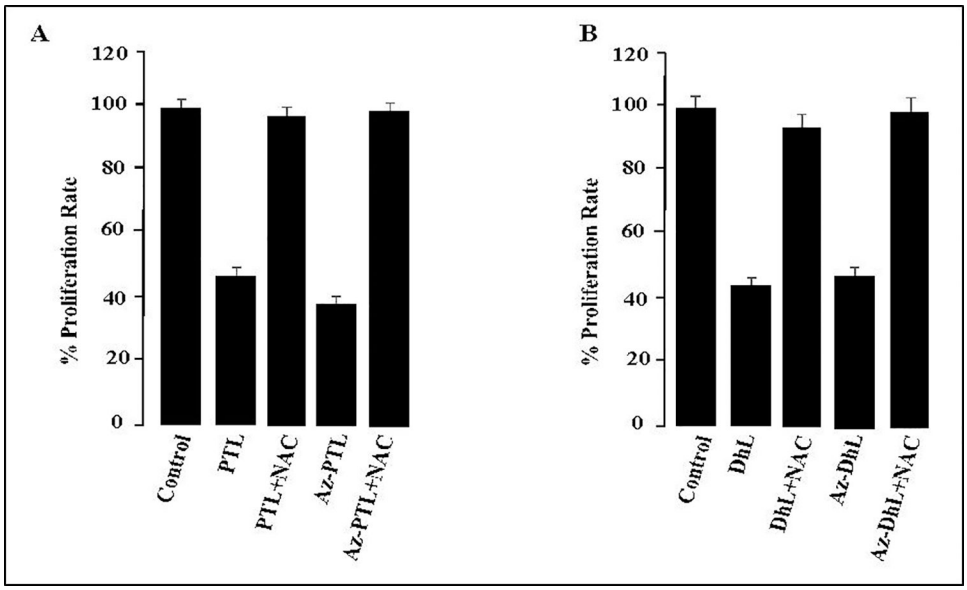

Figure 5.

NAC reverses the inhibitory effect of PTL, DhL, and their azido derivatives in MCF-7 cells. NAC (2 mM) was added to MCF-7 cells with 40 μM of PTL **1** and AzPTL **3** (Chart A) or DhL **2** and AzDhL **4** (Chart B). Each experiment was done in triplicate and expressed as +/− SEM.

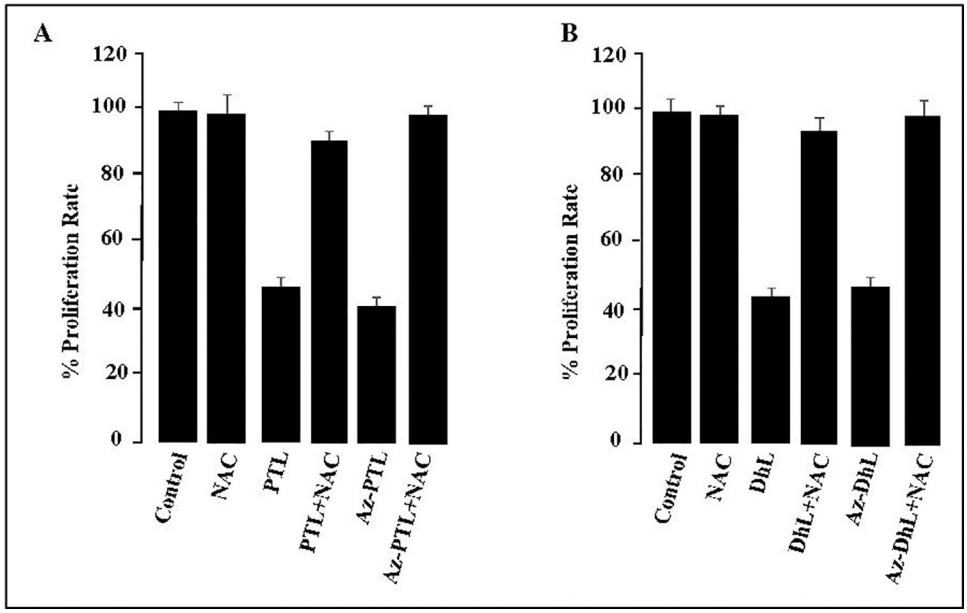

Figure 6.

NAC reverses the inhibitory effect of PTL, DhL, and their azido derivatives in MDA-MB-231 cells. NAC (2 mM) was added to MDA-MB-231 cells alone, with 40 μM of PTL **1** and AzPTL **3** (Chart A) or DhL **2** and AzDhL **4** (Chart B). Each experiment was done in triplicate and expressed as +/− SEM.

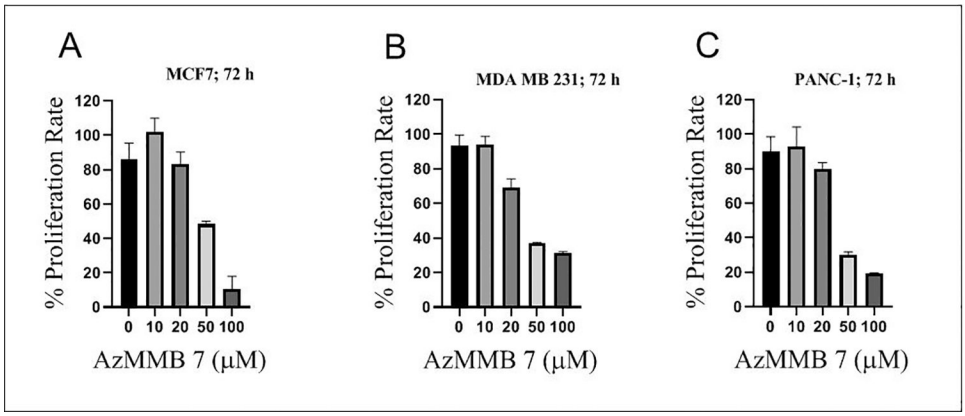

Figure 7.

AzMMB suppresses (A) MCF-7, (B) MDA-MB-231, and (C) PANC-1 cells proliferation in a dose-dependent manner at 72 h.

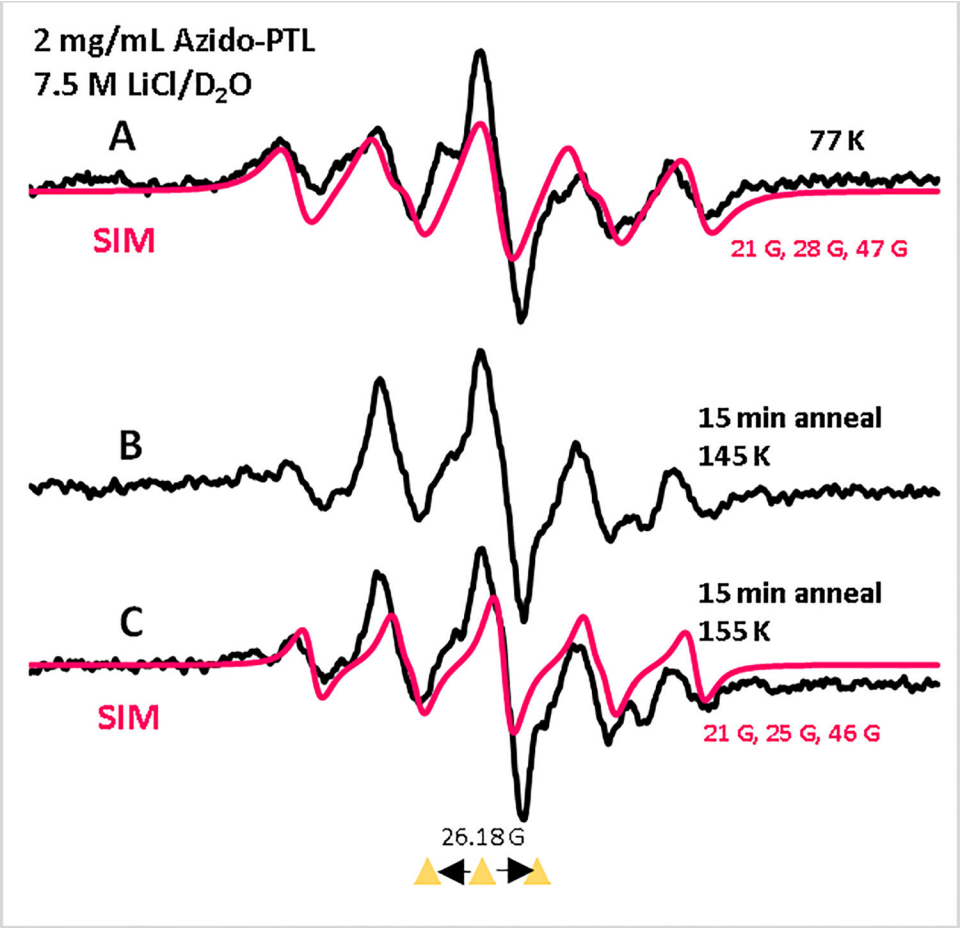

Figure 9.

ESR spectra of γ-irradiated (absorbed dose = 500 Gy at 77 K) homogeneous glassy solution of AzPTL **3** (2 mg/mL, black) in 7.5 M LiCl in D_2O (A) at 77 K. Spectra A through C are assigned to radical **9** formed as depicted in Scheme 4. Spectra (B, black) and (C, black) were obtained via stepwise annealing of the sample for 15 min at ca. 145 and ca. 155 K in the dark. The black spectra in A and B were obtained after subtraction of the line components of $Cl_2^{\bullet-}$ spectrum, following our previous works,[25, 27] from the individual experimentally recorded spectrum. The spectra (red) are the simulated spectra (for simulation parameters, see SI section). Three equally spaced (13.09 G) reference triangles in this Figure and in subsequent Figures show Fremy's salt resonances with central marker at $g = 2.0056$.

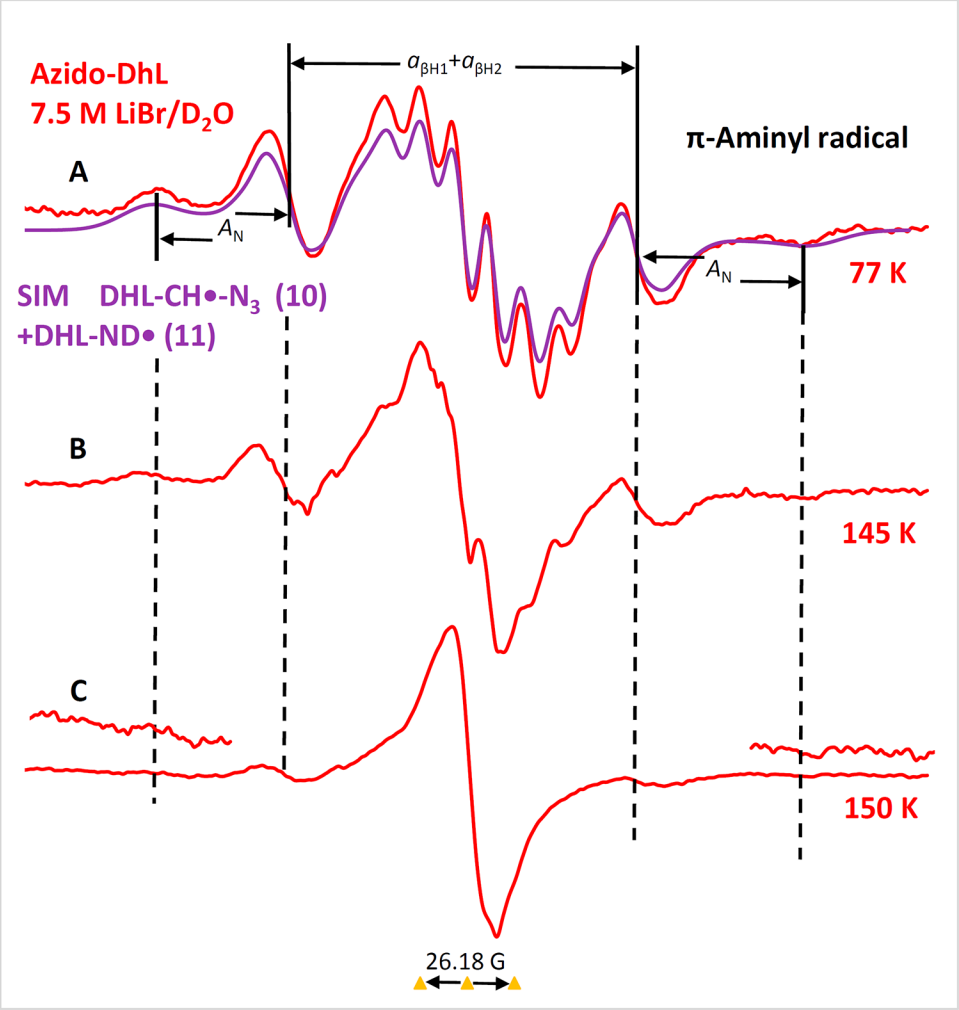

Figure 10.

(A) ESR spectrum (red) after radiation-produced one-electron addition to AzDhL **4** (2.0 mg/mL) at 77 K (γ-irradiation, 500 Gy) in 7.5 M LiBr/D_2O in dark; the violet spectrum is the combination of the simulated spectra of radicals **10** and **11** respectively (for simulation details including parameters see SI section; Figure S5 and S7–S9). Spectra shown in B and C were obtained via stepwise warming of the sample for 15 min at ca. 145 K and at ca. 150 K in the dark. The spectra at the wings in Figure C were multiplied by 5. All spectra were recorded at 77 K.

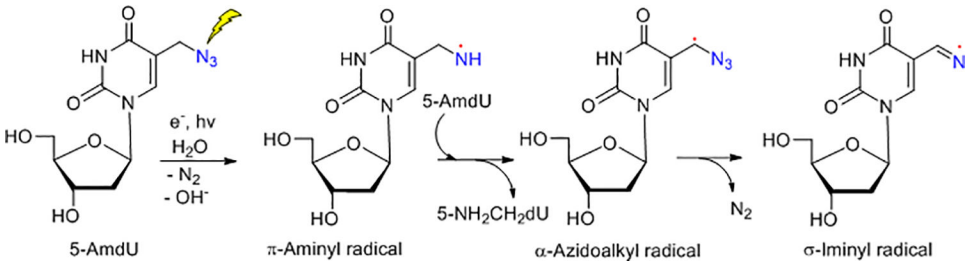

Scheme 1.

Radiation-produced electron-mediated site-specific formation of the neutral aminyl and iminyl radical from 5-AmdU via DEA.[25]

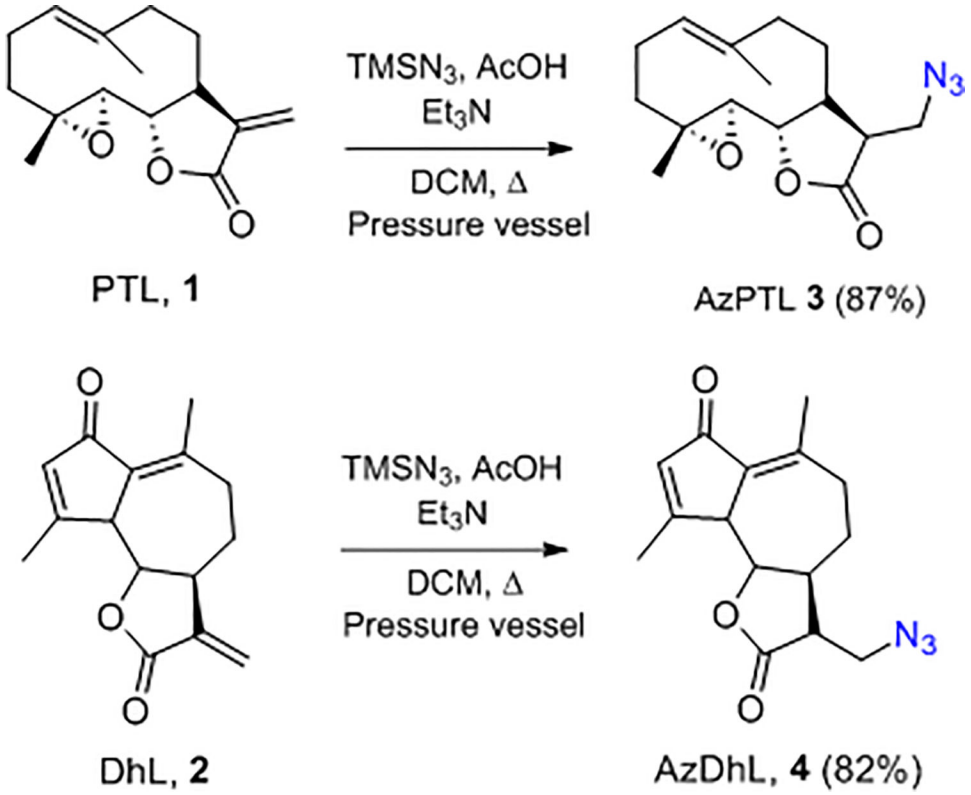

Scheme 2.
Synthes of AzPTL **3** and AzDhL **4** (1st generation AzSLs).

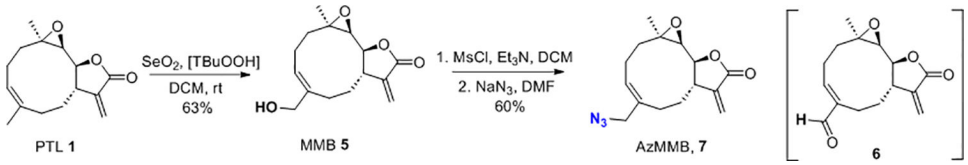

Scheme 3.
Synthesis of AzMMB **7** (2nd generation AzSLs).

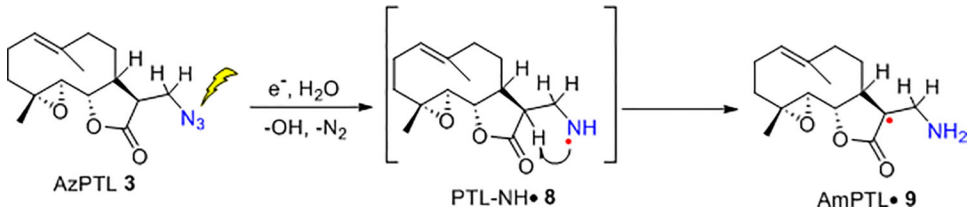

Scheme 4.

Intramolecular formation of the neutral tertiary carbon-centered radical AmPTL• **9** from AzPTL.

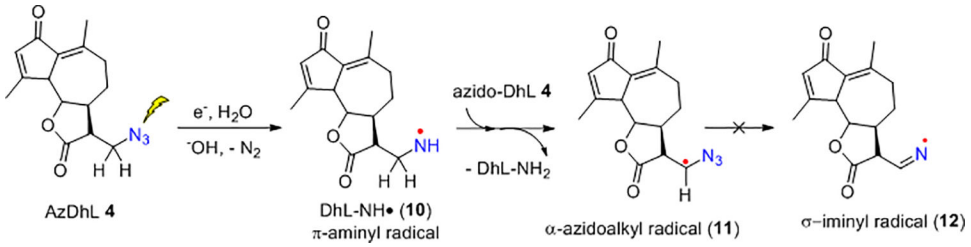

Scheme 5.

Formation of α-azidoalkyl radical **11** from AzDhL **4**.